

Time optimal path planning in stochastic dynamic flows

Manmeet Bhabra, Manan Doshi

December, 2019

1 Introduction

Autonomous underwater and surface vehicles have become increasingly prevalent in ocean applications in recent years. From military surveillance to scientific applications involving data collection, these vehicles provide a much more cost and time effective approach to traditional methods from the past. A central task in the operation of AUVs is in the generation of paths that optimize some predefined metrics, such as minimization of time or expenditure of energy, for the vehicles to follow when moving from checkpoint to checkpoint. A key issue however in this path generation process is that the ocean, due to the presence of strong and dynamic external flow fields, poses a challenge in determining these vehicle trajectories. More often than not, the order of magnitude of ocean currents is comparable to the relative velocity of these small vehicles, thus resulting in the currents having a non-negligible impact on the vehicle dynamics. What complicates matters even more is the fact that ocean current and velocity field forecasts are highly uncertain, thus making the problem inherently a stochastic one in which risk must be considered.

In this work, we look to build upon the schemes presented in [1, 2, 3], which address this very problem of time-optimal path planning in dynamic ocean environments through the use of the level set method. We moreover look to couple these approaches with a very popular procedure in stochastic ocean applications: data assimilation. In particular, by using efficient data assimilation schemes, we investigate in this work an on-board path planning algorithm that, on the fly, computes the path of the vehicle while also using data collected along the way to reduce the overall uncertainty in the flow fields. In this way, as the vehicle becomes more certain about its environment, it is able to effectively navigate to its destination. As such, our goal in this work is two-fold - reach the target with minimal risk (by learning as much as possible about the environment) and reach the target quickly.

2 Problem Statement

We begin by first describing in detail the problem statement. Consider a vehicle in a physical domain Ω and an uncertain nonlinear dynamic flow field $\mathbf{V}(\mathbf{x}, t; \omega)$. The vehicle has, as its control, the heading at which it can move, $\hat{\mathbf{h}}(t)$ (note that the speed with which to move relative to the water, F , will also generally be a control for the vehicle but in this work we assume it to be constant). Furthermore, let us denote the start point and the desired final position of the vehicle as \mathbf{x}_s and \mathbf{x}_f , respectively. The governing equations for the dynamics of the vehicle are given as

$$\frac{d\mathbf{x}(t;\omega)}{dt} = F \cdot \hat{\mathbf{h}}(t) + \mathbf{V}(\mathbf{x}, t; \omega) \quad (1)$$

Note that in equation (1), the controls provided to the vehicle are deterministic, however due to the uncertain velocity field the resulting path followed, $\mathbf{x}(t; \omega)$, will be uncertain. Our goal is to determine this set of headings so as to navigate the vehicle from \mathbf{x}_s to \mathbf{x}_f (more specifically, to reach close to the final desired destination with high enough probability) in the uncertain environment, while also being as time optimal as possible.

It is straightforward that, given less uncertainty about the velocity field, the vehicle will be able to generate, and follow, an optimal path to the destination with much less difficulty and risk. In light of this, the additional objective we look to tackle is to efficiently reduce the uncertainty in the flow field as the vehicle proceeds towards the destination. That is, given a prior distribution over the stochastic variables that parameterizes $\mathbf{V}(\mathbf{x}, t; \omega)$, we look to use measurements of the position data of the vehicle to obtain a posterior for these random variables that reduces the overall uncertainty in the problem. In this way, as the mission progresses and the vehicle starts to traverse through the environment and collect data about itself, the inherent risk continues to decrease.

Furthermore, we summarize the following key assumptions that will be used in this work for the cases considered:

- The vehicle is assumed to move as a point mass and as such not exhibit any inertia in its motion.
- We assume that the flow field is smooth and differentiable. Moreover, in all cases, we have considered fields with parametric, closed form formulations. In future work, we will look to handle more complicated domains where no closed form solution exists and, as such, the full Navier-Stokes equations must be solved to obtain the velocity field.
- Uncertainty in the environment is only considered in the velocity flow field. No obstacles (such as islands or coastal regions) were considered. In future work, we will look to incorporate these features as well.

3 Time Optimal Path Planning for Strong Deterministic and Stochastic Dynamic Flows

3.1 Deterministic Flows

We start by first, in this section, outlining the key approach used to solve the deterministic time-optimal path problem. For additional details, we refer the reader to [1, 4, 5, 6, 7].

Central to the process of computing the time-optimal path is the accurate evolution of what is known as the reachability set of the vehicle starting from the defined start point. In control theory, the reachability set refers to the set of all points in the physical space that a vehicle can reach within a given time period. The boundary of this set is aptly termed the reachability front, and it intuitively corresponds to the furthest points in space the vehicle could reach at a given time. Framed using the concept of reachability sets the time optimal

path problem is then simple: continue to evolve the reachability front until it touches the target. The resulting path followed by a point that remained on the front and reached the target is then the corresponding time-optimal path.

To numerically evolve the reachability front, an efficient scheme is needed. Representing the front using a set of discrete points is one approach, however, once the reachability set is evolved, these points will generally tend to cluster in some regions and spread apart in others, thus providing an insufficient parametrization. An alternate, and much more efficient, approach is to use the level set method. Consider a domain $\mathbf{x} \in \mathbb{R}^d$. The level set of a function $\phi(\mathbf{x})$ is the set given by $\{\mathbf{x} : \phi(\mathbf{x}) = C\}$ where C is some defined constant. This level surface is moreover a hyper-surface of dimension \mathbb{R}^{d-1} embedded in the domain. The key concept in the level set method is to represent the reachability front (which is a hyper-surface of dimension \mathbb{R}^{d-1}) by a level surface of some function $\phi(\mathbf{x})$ (typically the zero-contour is used). In doing so, the problem of evolving the reachability front translates into one of evolving the function $\phi(\mathbf{x})$.

We now introduce the key equations used to evolve the reachability front of the vehicle. Denote by $\phi(\mathbf{x}, t)$ a function such that its zero-contour ($\{x : \phi(\mathbf{x}, t) = 0\}$) gives the reachability front of the vehicle at a time t . Moreover, the reachability set at any time t is defined as $\{x : \phi(\mathbf{x}, t) < 0\}$. The initial condition for the implicit function is moreover set as $\phi(\mathbf{x}, t = 0) = \phi_0$, where ϕ_0 corresponds to the initial reachability front of the vehicle (this is typically taken to be given by $\phi(\mathbf{x}, t = 0) = \|\mathbf{x} - \mathbf{x}_s\|$). Given the deterministic version of the vehicle dynamics in equation (1), the evolution of the reachability front can be shown to be governed by the following partial differential equation [1]:

$$\frac{\partial \phi(\mathbf{x}, t)}{\partial t} + F |\nabla \phi(\mathbf{x}, t)| + \mathbf{V}(\mathbf{x}, t) \cdot \nabla \phi(\mathbf{x}, t) = 0, \quad \phi(\mathbf{x}, t = 0) = \phi_0 \quad (2)$$

Equation (2) (which we refer to in this paper as the level set equation) may be discretized (any traditional technique such as finite differences, finite volumes and finite elements can be used) and solved numerically until the time t_f such that $\phi(\mathbf{x}_f, t_f) = 0$. That is, the equation is solved until the reachability front reaches the target.

Once the reachability front has reached the destination, it still remains to determine the optimal path to be followed by the vehicle. It can be shown (refer to [1]) that, given a vehicle on the reachability front, the optimal heading to take is to move normal to the reachability front: $\mathbf{h}(t) = \frac{\nabla \phi(\mathbf{x}, t)}{|\nabla \phi(\mathbf{x}, t)|}$. Using this fact, the optimal path can then be efficiently determined using the evolved level set $\phi(\mathbf{x}, t)$ by solving backwards in time from the destination to the target. Specifically, the optimal path, $\mathbf{x}_p(t)$, can be shown to be governed by the ODE given as

$$\frac{d\mathbf{x}_p(t)}{dt} = -\mathbf{V}(\mathbf{x}, t) - F \frac{\nabla \phi(\mathbf{x}, t)}{|\nabla \phi(\mathbf{x}, t)|} \quad (3)$$

which is solved backward in time starting from $\mathbf{x} = \mathbf{x}_f$ and time $t = t_f$. Equation (3) is referred to as the backtracking equation.

3.2 Stochastic Flows

In the stochastic counterpart of the preceding analysis we consider an uncertain flow field of the form $\mathbf{V}(\mathbf{x}, t; \omega)$ where we have considered a probability space $(\Omega, \mathcal{B}, \mathcal{P})$ and $\omega \in \Omega$. The stochastic time-optimal path planning problem is then solved through considering a stochastic reachability front $\phi(\mathbf{x}, t; \omega)$ that evolves according to the stochastic version of equation (2):

$$\frac{\partial \phi(\mathbf{x}, t; \omega)}{\partial t} + F |\nabla \phi(\mathbf{x}, t; \omega)| + \mathbf{V}(\mathbf{x}, t; \omega) \cdot \nabla \phi(\mathbf{x}, t; \omega) = 0, \quad \phi(\mathbf{x}, t = 0; \omega) = \phi_0 \quad (4)$$

Moreover, the corresponding stochastic backtracking equation used to find the optimal paths is given as

$$\frac{d\mathbf{x}_p(t; \omega)}{dt} = -\mathbf{V}(\mathbf{x}, t; \omega) - F \frac{\nabla \phi(\mathbf{x}, t; \omega)}{|\nabla \phi(\mathbf{x}, t; \omega)|} \quad (5)$$

Many schemes exist to solve stochastic PDEs and ODEs. In this work, however, we consider the standard Monte Carlo method as a first step to test the effectiveness of our approach. For further details, we refer the reader to [2, 3].

4 Data Assimilation

Data assimilation is a process used to estimate dynamic fields by combining information from observations and those produced through predictions from computational models. In essence, discrepancies between computational model predictions (which uses an assumed dynamic field) and these observations allows for the ability to obtain a richer estimate of the underlying field.

We consider in this work inversion processes that fall into the rich field of Bayesian filtering. Consider some hidden state \mathbf{X} that is the subject of inversion. To infer information about this state, the practitioner instills a prior (ideally an informed one that uses some approximate or predefined knowledge of the problem) on this state: $p_{\mathbf{X}}(\mathbf{x})$. A measurement model is then assumed which relates the measurements/observations, \mathbf{Y} , to the hidden states of interest. This model can then be used to form the likelihood, $p_{\mathbf{Y}|\mathbf{X}}(\mathbf{y}|\mathbf{x})$, which corresponds to how probable a given measurement is given some fixed hidden state. Through the knowledge of these two components, the posterior $p_{\mathbf{X}|\mathbf{Y}}(\mathbf{x}|\mathbf{y})$ can then be formed which gives a richer estimate for the hidden state given the data [8].

In this section, we outline two main filtering approaches used in this work: (1) the GMM Filter and (2) the Ensemble Kalman Filter (EnKF).

4.1 The GMM Filter

The first filtering approach we investigate is based upon the Gaussian Mixture Model (GMM). Consider a random variable given by $\mathbf{X} \in \mathbb{R}^n$ distributed according to a GMM. It's pdf can then be written compactly as:

$$p_{\mathbf{X}}(\mathbf{x}) = \sum_{i=1}^M \pi_i \cdot \mathcal{N}(\mathbf{x}; \boldsymbol{\mu}_i, \mathbf{P}_i) \quad (6)$$

where M corresponds to the number of mixture components used (also known as the complexity of the GMM), $\mathcal{N}(\mathbf{x}; \boldsymbol{\mu}_i, \mathbf{P}_i)$ are Gaussian pdfs (with mean $\boldsymbol{\mu}_i$ and covariance \mathbf{P}_i) and π_i are weights corresponding to each Gaussian with the requirement that

$$\sum_{i=1}^M \pi_i = 1. \quad (7)$$

GMMs are quite popular in Bayesian methods due to the simplicity that results from the normal distribution in inversion. For instance, the Gaussian distribution is a conjugate prior for observation models that are Gaussian (which is typically what is assumed in practice). Specifically, given a random variable \mathbf{X} with a prior as given in equation (6) and a likelihood model as given by

$$p_{\mathbf{Y}|\mathbf{X}}(\mathbf{y}|\mathbf{x}) = \mathcal{N}(\mathbf{y}; \mathbf{H} \cdot \mathbf{x}, \mathbf{R}) \quad (8)$$

the posterior $p_{\mathbf{X}|\mathbf{Y}}(\mathbf{x}|\mathbf{y})$ is also a GMM with components given as:

$$p_{\mathbf{X}|\mathbf{Y}}(\mathbf{x}|\mathbf{y}) = \sum_{i=1}^M \hat{\pi}_i \cdot \mathcal{N}(\mathbf{x}; \hat{\boldsymbol{\mu}}_i, \hat{\mathbf{P}}_i) \quad (9)$$

$$\hat{\boldsymbol{\mu}}_i = \boldsymbol{\mu}_i + \mathbf{K}_i(\mathbf{y} - \mathbf{H} \cdot \boldsymbol{\mu}_i) \quad (10)$$

$$\hat{\mathbf{P}}_i = (\mathbf{I} - \mathbf{K}_i \cdot \mathbf{H}) \cdot \mathbf{P}_i \quad (11)$$

$$\hat{\pi}_i = \frac{\pi_i \cdot \mathcal{N}(\mathbf{y}; \mathbf{H} \cdot \boldsymbol{\mu}_i, \mathbf{H} \mathbf{P}_i \mathbf{H}^T + \mathbf{R})}{\sum_{k=1}^M \pi_k \cdot \mathcal{N}(\mathbf{y}; \mathbf{H} \cdot \boldsymbol{\mu}_k, \mathbf{H} \mathbf{P}_k \mathbf{H}^T + \mathbf{R})} \quad (12)$$

where \mathbf{K}_i corresponds to the Kalman gain and is given as:

$$\mathbf{K}_i = \mathbf{P}_i \mathbf{H}^T [\mathbf{H} \mathbf{P}_i \mathbf{H}^T + \mathbf{R}]^{-1}. \quad (13)$$

Even though such efficient rules exist for obtaining posterior GMMs, these would be severely limited if there were no efficient way to obtain GMMs of ensembles of particles. Fortunately, such an approach does exist and is known commonly as the Expectation-Maximization algorithm. This algorithm provides an efficient iterative procedure to, given a set of N realizations of some random variable $\{\mathbf{x}\}_{i=1}^N$, obtain the corresponding GMM that fits the data the best it can (commonly known as the maximum likelihood estimate). As a result, given an ensemble of realizations and the corresponding GMM fit to it, a new observation, \mathbf{y} , may then be used to efficiently obtain the posterior using equations (12), (10) and (11). For further details regarding the GMM and its use in filtering, we refer the reader to [9, 10, 8].

4.2 The Ensemble Kalman Filter

The Ensemble Kalman Filter (EnKF) is another widely used approach in data assimilation. Due to its robustness, ease of implementation and accuracy, the EnKF has been prevalent in numerous applications ranging from oceanography to weather forecasting. The EnKF moreover may be extended from its traditional form to be used for solving inverse problems. The details for this approach can be found in [11].

Consider a model with an unknown parameter \mathbf{X} . Moreover, let the forward model be denoted by \mathcal{G} . Using these, we can predict data obtained from the system as:

$$\underbrace{\mathbf{Y}}_{\text{'Data'}} = \underbrace{\mathcal{G}}_{\text{Forward Model}} \left(\underbrace{\mathbf{X}}_{\text{Model Parameters}} \right) + \underbrace{\boldsymbol{\eta}}_{\text{Noise}} \quad (14)$$

The key goal in the inverse problem is to predict the model parameter $\mathbf{X} \in \mathcal{X}$ given the observation $\mathbf{Y} \in \mathcal{Y}$. To perform the inversion, we consider an initial ensemble of the model parameter \mathbf{x}_i distributed according to the prior belief of that parameter, $p_{\mathbf{X}}(\mathbf{x})$. Next, consider an augmented state variable $\mathbf{X}_{aug} \in \mathcal{X} \times \mathcal{Y}$. We define the system for our augmented state as:

$$\mathbf{X}_{aug} = \begin{bmatrix} \mathbf{X} \\ \mathbf{Y} \end{bmatrix}$$

$$\mathbf{x}_{aug,t+1} = \mathbb{F}(\mathbf{x}_{aug,t}) \quad \text{Where } \mathbb{F}(\mathbf{x}_{aug}) = \begin{bmatrix} \mathbf{x} \\ \mathcal{G}(\mathbf{x}) \end{bmatrix} \quad (15)$$

$$\mathbf{y}_t = \mathbf{H} \cdot \mathbf{x}_{aug,t} + \boldsymbol{\eta}_t \quad \text{Where } \mathbf{H} = \begin{bmatrix} \mathbf{0} & \mathbf{I} \end{bmatrix}$$

On applying the Ensemble Kalman Filter on this system, one obtains a posterior for the model parameters and observations represented through a set of realizations (an ensemble). The general algorithm for the EnKF is described in Algorithm (1). For this project, we have implemented the basic one step *ENKFR* approach as detailed in [11].

Algorithm 1: Algorithm for the Ensemble Kalman Filter

Input: Initial Ensemble $z_0^{(j)}$, Observations y , Noise covariance R for η
Result: The posterior ensemble of the state given the data

```

/* Initialization */
1 t = 1
2
/* Prediction Step */
3  $\hat{z}_t^{(j)} = \mathbb{F}(z_{t-1}^{(j)})$  // Prediction Ensemble
4  $\bar{z}_t = \frac{1}{J} \sum_j \hat{z}_t^{(j)}$  // Mean Prediction
5  $C_t = \text{cov}(\hat{z}_t)$  // Covariance of ensemble
6
/* Analysis Step */
7  $K_t = C_t H^T (H C_t H^T + R)^{-1}$  // Kalman Gain
8  $y_t^{(j)} = y + \eta_t^{(j)}$  // Perturbed observations
9  $z_t^{(j)} = \hat{z}_t^{(j)} + K_t (y_t^{(j)} - H \hat{z}_t^{(j)})$  // The required posterior

```

5 Risk Aware Time-Optimal Path Planning in Strong Stochastic Dynamic Flows

5.1 General Approach

With the basics of the stochastic time-optimal path planning problem and data assimilation procedures outlined in Sections 3 and 4, we now describe our approach to merge these methods to allow for risk aware path planning.

Consider once again the problem of navigating an AUV from a start point \mathbf{x}_s to its final destination \mathbf{x}_f in an environment with a strong uncertain dynamic flow field $\mathbf{V}(\mathbf{x}, t; \omega)$. Approaches exist for computing offline a distribution of different optimal paths in this environment using equations (4) and (5), however then choosing which path to feed to the vehicle to take is a challenge. Clearly, choosing and taking a fixed path using this distribution (such as the maximum probability or mean path) using only the limited prior knowledge of the velocity field will be inadequate in general situations.

Due to this, we consider an approach inspired loosely on model predictive control. Rather than navigating the vehicle directly from the start to the end point, we consider the process of controlling the vehicle in sequences of finite time horizons. We then use data collected at the end of each time horizon, and our chosen data assimilation method, to refine our estimate of the environment. As the knowledge of the environment changes, new paths are then computed on the fly and followed by the vehicle. As a result, the original off-line path planning problem becomes an on-board one where the vehicle continuously charts out its own path using updated knowledge from data it has acquired.

We outline now in detail the key steps involved in this hybrid data assimilation - path planning approach. Consider for simplicity a velocity field $\mathbf{V}(\mathbf{x}, t, \boldsymbol{\xi})$ parametrized by a vector of random variables $\boldsymbol{\xi}$. We consider, moreover, a prior $p_{\boldsymbol{\xi}}(\boldsymbol{\xi})$ on these random variables. The path planning problem is started by first choosing the most likely (maximum probability) realization of $\boldsymbol{\xi}$, denoted by $\boldsymbol{\xi}_{MP}$, which ultimately is associated with the most likely velocity field $\mathbf{V}(\mathbf{x}, t, \boldsymbol{\xi}_{MP})$. The deterministic level set and backtracking equation is then solved for this velocity field to obtain a candidate optimal path $\mathbf{x}_{p,MP}(t)$ starting from the point \mathbf{x}_s at time t_s and terminating at the destination \mathbf{x}_f and time t_f . The sequence of headings contained in this candidate optimal path, over a time horizon Δt_h , is then considered for the uncertain velocity fields to obtain a distribution of possible final position of the AUV at the end of the time horizon: $p_{\mathbf{X}_{t_s+\Delta t_h}}(\mathbf{x}_{t_s+\Delta t_h})$. The time horizon Δt_h is adaptively chosen as the time taken for the actual path to stray away from the candidate optimal path by a certain predefined value.

With the distribution of possible final positions, we now outline how the assimilation proceeds. Feeding the chosen set of headings from $\mathbf{x}_{p,MP}(t)$ over the time horizon $[t_s, t_s + \Delta t_h]$ to the real life vehicle we obtain a measurement for the final position at the end of the horizon $\mathbf{y}_{t_s+\Delta t_h}$. Now define a new augmented random state variable as

$$\mathbf{X}_{aug} = \begin{bmatrix} \boldsymbol{\xi} \\ \mathbf{x}_{t_s+\Delta t_h} \end{bmatrix}, \quad (16)$$

The joint prior $p_{\mathbf{X}_{aug}}(\mathbf{x}_{aug})$ can be found using the priors $p_{\mathbf{X}_{t_s+\Delta t_h}}(\mathbf{x}_{t_s+\Delta t_h})$ and $p_{\boldsymbol{\xi}}(\boldsymbol{\xi})$. Fur-

thermore, consider a Gaussian measurement model relating the augmented state to the measurements of the following form

$$\mathbf{Y} = \mathbf{H} \cdot \mathbf{X}_{aug} + \boldsymbol{\epsilon}, \quad (17)$$

where $\boldsymbol{\epsilon} \sim \mathcal{N}(\boldsymbol{\epsilon}; 0, \mathbf{R})$ is the assumed noise in the measurement which is taken to be normally distributed. The matrix \mathbf{H} is moreover given as:

$$\mathbf{H} = \begin{bmatrix} \mathbf{0}_{n_\xi} & \mathbf{0} \\ \mathbf{0} & \mathbf{I}_{n_x} \end{bmatrix}. \quad (18)$$

Using the prior $p_{\mathbf{X}_{aug}}(\mathbf{x}_{aug})$ and likelihood (found using the measurement model) $p_{\mathbf{Y}|\mathbf{X}_{aug}}(\mathbf{y}|\mathbf{x}_{aug})$, the filtering procedures, as outlined in Section 4, may be used to obtain $p_{\mathbf{X}_{aug}|\mathbf{Y}}(\mathbf{x}_{aug}|\mathbf{y})$. This posterior distribution for the augmented state can then be marginalized to yield a posterior estimate for the uncertain flow field variables $\boldsymbol{\xi}$.

The previous steps outlined in detail the assimilation process over the first time horizon when the vehicle leaves the start position \mathbf{x}_s . For the next horizon, we effectively repeat the whole process using the previously computed posterior for $\boldsymbol{\xi}$ as a new prior and starting now from the previously obtained measurement for the vehicle's position $\mathbf{y}_{t_s+\Delta t_h}$ instead of \mathbf{x}_s . We continuously repeat this process until the vehicle is sufficiently close to the destination. At the end of each time horizon, the uncertainty in $\boldsymbol{\xi}$ gets smaller and smaller, thus improving our knowledge of the flow field and reducing the overall risk of navigation. Furthermore, the pseudo-code this procedure is outlined in Algorithm (2).

It is moreover important to point out that, due to uncertainty, the obtained path will not necessarily be time-optimal. Instead, we hope to approach time-optimality as closely as possible by repeatedly considering these trajectories from each intermediary state of the vehicle after each time horizon.

Algorithm 2: Coupled Time-Optimal Path Planning with Data Assimilation Procedure

Result: Path to the destination in the uncertain flow field

```
1 while true do
  /* At the start of this step, use the prior for the random variable  $\xi$  that
   parametrizes the flow and get the realization of the random variable that is
   most probable */
2   $\xi^* = \text{getMostProbableFlowVariable}()$ 
3
  /* Solve for the headings corresponding to the most probable optimal path */
4   $\text{optPathHeadings} = \text{solveOptimalPath}(\xi^*)$ 
5
  /* Using Monte Carlo, evolve vehicle states for ocean realizations using set of
   optimal paths over a time horizon. Obtain ensembles of final positions of
   vehicles */
6   $X_{ensembles} = \text{forwardSolveVehiclesMonteCarlo}(\text{optPathHeadings}, \Delta t_{horizon})$ 
7
  /* Send the same controls to the real vehicle and obtain a measurement for its
   final position */
8   $Y_{measurement} = \text{moveRealVehicle}(\text{optPathHeadings}, \Delta t_{horizon})$ 
9
  /* Use the vehicles position and the ensembles to assimilate the true velocity
   field flow variables. We will use this posterior for  $\xi$  in the next pass
   through the loop */
10  $\text{assimilateFlow}(X_{ensembles}, Y_{measurement})$ 
11
  /* Check if we have reached the destination. If not, repeat the loop */
12 if Destination is reached then
13   | break
14 end
15 end
```

6 Results

6.1 Double Gyre (Uncertain A)

We first test our method on the oscillating asymmetrical double gyre flow. The equations governing the dynamics of the flow are given as:

$$\begin{aligned} f(x, t) &= a(t)x^2 + b(t)x \\ a(t) &= \epsilon \sin(\omega t) \\ b(t) &= 1 - 2\epsilon \sin(\omega t) \\ u &= -\frac{\partial \psi}{\partial y} = -\pi A \sin(\pi f(x)) \cos(\pi y) \\ v &= \frac{\partial \psi}{\partial x} = \pi A \cos(\pi f(x)) \sin(\pi y) \frac{df}{dx} \end{aligned} \tag{19}$$

This is a flow consisting of two gyres of unequal size separated by an interface. The interface, moreover, pulsates with a time period of 2 units thus resulting in the gyres changing size with time in a periodic manner. The two extreme configurations reached in one time period are plotted in Figure 1.

In this case, we consider an uncertain strength of the flow, A . In Equation 19, A is

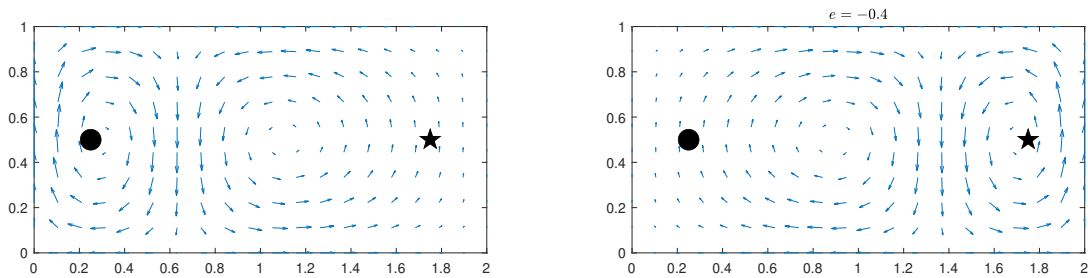


Figure 1: The two extreme flows reached in one time period for the double gyre flow field.

thus treated as a random variable. We consider the prior to be a Gaussian with mean 0 and standard deviation 0.1. The true value of A hidden to the algorithm is 0.1. Furthermore, since the max vehicle speed is just 0.4, this is a very strong dynamic flow.

Figure (2) depicts the paths obtained from our procedure when using the GMM filter and EnKF. We show in green first the path followed by the real vehicle in the true environment. The red points moreover correspond to points at which an assimilation step is completed. Furthermore, shown in the plot are also the ensemble of paths used in the assimilation. That is, following an assimilation step, once a proposed optimal path to the destination is computed, the effect of using the controls for this path over a limited time horizon are considered in each flow field realization (different realizations of A). This collection of paths, following each assimilation step, are what are shown in the figure. To perform the assimilation, the end points of these paths are effectively compared to the measured position of the real vehicle (the red point), and the filtering procedure as outlined in the preceding section is then used to obtain a posterior for A . As expected, before to the first assimilation step when the prior pdf for the flow field variable is used, there is a corresponding large spread in the resulting paths for the vehicles using the fixed controls in the different flow fields. However, following a few assimilation iterations, the vehicle has much more certainty about the flow field (the standard deviation of the distribution is much lower) and as such all the paths realizations can be seen to be quite close together.

Shown in Figure (3) is the evolution of the distribution over the random variable A after each assimilation step. It can be seen clearly that both filters are able to effectively converge close to the true hidden value for A within relatively few assimilation iterations. Predictably, an initial large correction is observed at the first assimilation step as the prior is quite far from the truth. This case thus provides a good demonstration of the capabilities of this procedure, as the vehicle was indeed able to navigate to the destination while also reducing the uncertainty in the environment.

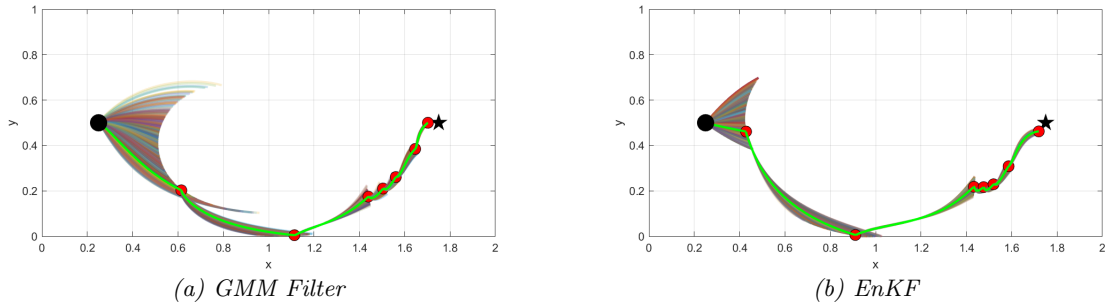


Figure 2: The evolution of the paths of the vehicle as predicted by the proposed approach for the case of an uncertain flow strength A in the double gyre flow field. Shown in green is the final path of the real vehicle in the true flow field. The red points correspond to locations at which an assimilation step was completed. The distribution of paths, following each assimilation step, results from considering the fixed set of controls in different flow field realizations. The discrepancy between the end point of these paths and the measured real vehicle locations in red is what is used to perform the assimilation.

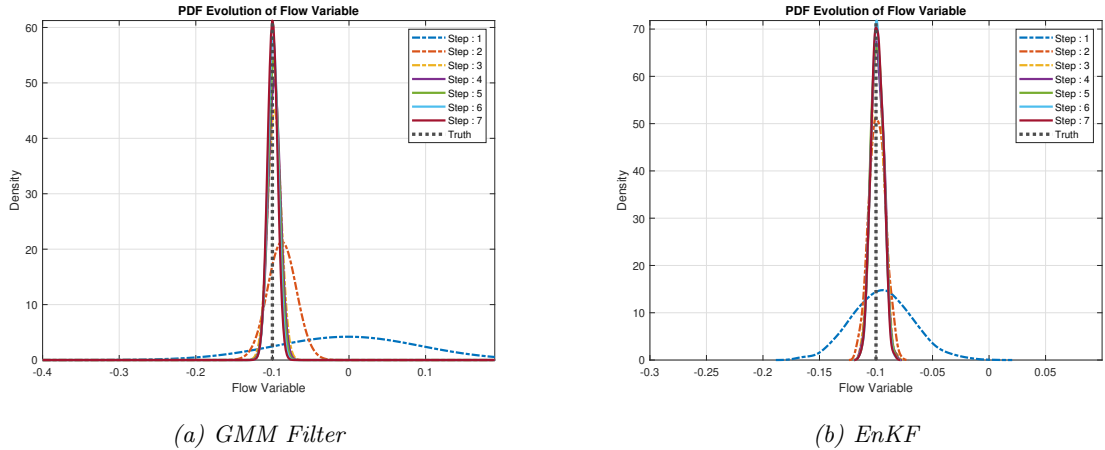


Figure 3: The evolving probability distribution functions for the stochastic A in our formulation (we plot the posterior pdf after each assimilation step). We can see that for both assimilation algorithms, the distribution converges to the correct value.

6.2 Double Gyre (Uncertain ϵ)

In the next case, we once more consider the double gyre but now fix the value of A and instead make ϵ the uncertain parameter. The flow is moreover considered to be steady with a fixed value of $t = 0.5$ in equation (19). Thus the flow is in the maximally perturbed state with an unknown amount of total perturbation. We do not know where the boundary between the two gyres is. Figure (4) shows the two possible realizations of the flow field for different values of ϵ : 0.4 and -0.4 . Figure (5) and (6) highlight that our proposed methodology is once again able to effectively navigate the vehicle to the destination while reducing the uncertainty in the environment.

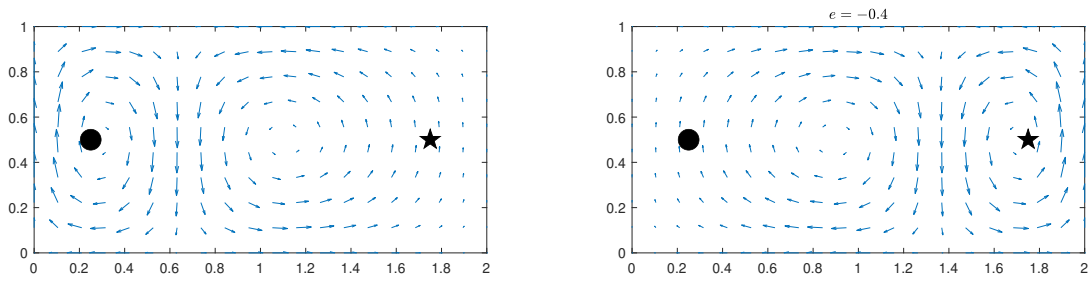


Figure 4: Examples of flow fields that can be reached by varying ϵ . Shown on the left is the flow field for $\epsilon = 0.4$ and shown on the right is one corresponding to $\epsilon = -0.4$.

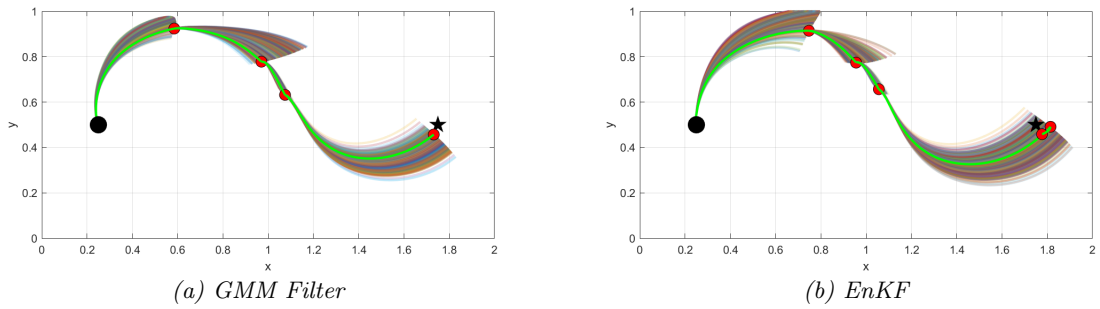


Figure 5: As in Figure (2) but for the case of an uncertain interface perturbation, ϵ , in the double gyre flow field equations.

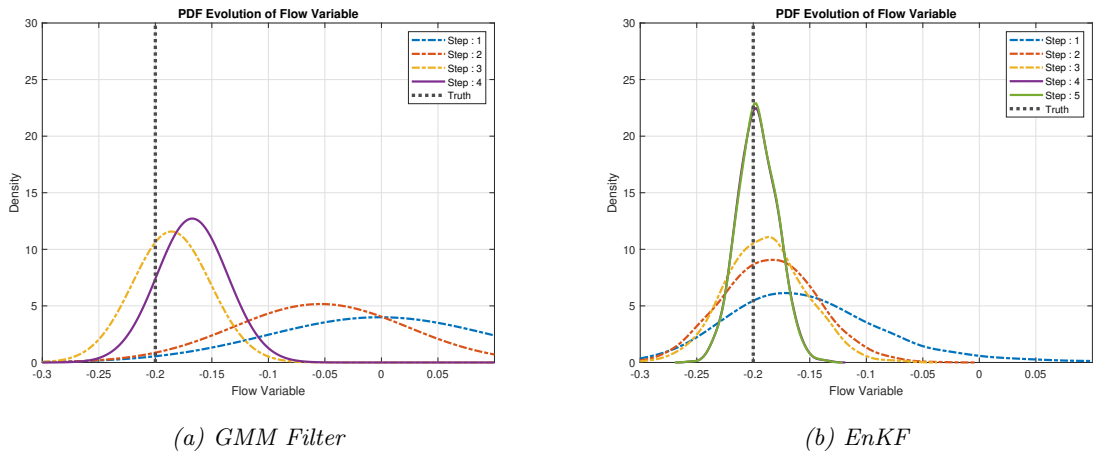


Figure 6: As in Figure (3) but for the case of an uncertain interface perturbation, ϵ .

7 Conclusions

In this work, we have considered a path planning scheme in uncertain dynamical flows that uses data assimilation to reduce uncertainty and risk. In particular, by using an approach based loosely on model predictive control, the global path planning problem is split up by considering

the motion of the vehicle over fixed time horizons. At the end of each time horizon, data collected from the vehicle is then used in an assimilation process to infer the underlying flow field. In this way, the vehicle becomes more and more informed about the uncertain environment after each time horizon and is able to therefore navigate more easily to the destination.

To verify the proposed scheme, two path planning cases in a complicated double gyre flow field were considered. Moreover, both the GMM filter and ENKF were investigated for the inversion process and all forward uncertainty propagation was completed using the Monte Carlo approach. For both stochastic flow cases, the proposed methodology was shown to successfully be able to navigate to the destination while simultaneously reducing the uncertainty in the environment as required.

8 Future work

Although a good start point, there are several points of improvement that we hope to address in future work regarding this method. To start, we plan to improve the approach used to solve the forward uncertainty propagation problem by using the Dynamically Orthogonal (DO) method [12, 13] instead of Monte Carlo. The DO method provides an efficient approach to solve the stochastic PDE/ODE by decomposing the solution into a deterministic mean field with a set of deterministic modes multiplied by a set of stochastic coefficients. We anticipate incorporating this method will result in a significant speed up in the computations and an increase in the accuracy.

Moreover, an additional approximation made in the analysis was the treatment of the stochastic position of the vehicle after each time horizon. At the end of each time horizon, a posterior for the position of the vehicle would be obtained. However, for subsequent time steps, for simplicity, the path planning problem would be initialized from the measured vehicle position and this posterior distribution would not be used in order to remain computationally tractable. In future work, we would look to effectively compute the evolution of optimal paths originating from these uncertain positions, and then use these to formulate an approach to choose a path for the vehicle to follow while simultaneously performing the assimilation.

Finally, the assimilation step can also be improved by using, instead of only the final state at the end of each time horizon, the whole path between horizons (i.e. the collection of states) to perform the inversion. This collection of states clearly adds additional information to the assimilation process and would most likely help obtain much larger drops in the overall uncertainty much quicker.

References

- [1] T. Lolla, M. P. Ueckermann, K. Yigit, P. J. Haley, and P. F. J. Lermusiaux, “Path planning in time dependent flow fields using level set methods,” in *2012 IEEE International Conference on Robotics and Automation*, pp. 166–173. ISSN: 1050-4729, 1050-4729, 1050-4729.
- [2] D. N. Subramani, Q. J. Wei, and P. F. J. Lermusiaux, “Stochastic time-optimal path-planning in uncertain, strong, and dynamic flows,” vol. 333, pp. 218–237.

- [3] D. N. Subramani and P. F. J. Lermusiaux, “Risk-optimal path planning in stochastic dynamic environments,” vol. 353, pp. 391–415.
- [4] S. V. T. Lolla, *Path planning and adaptive sampling in the coastal ocean*. PhD thesis, Massachusetts Institute of Technology, 2016.
- [5] T. Lolla, P. F. Lermusiaux, M. P. Ueckermann, and P. J. Haley, “Time-optimal path planning in dynamic flows using level set equations: theory and schemes,” *Ocean Dynamics*, vol. 64, no. 10, pp. 1373–1397, 2014.
- [6] T. Lolla, P. J. Haley, and P. F. Lermusiaux, “Time-optimal path planning in dynamic flows using level set equations: realistic applications,” *Ocean Dynamics*, vol. 64, no. 10, pp. 1399–1417, 2014.
- [7] C. S. Kulkarni, *Three-dimensional time-optimal path planning in dynamic and realistic environments*. PhD thesis, Massachusetts Institute of Technology, 2017.
- [8] S. Särkkä, *Bayesian filtering and smoothing*, vol. 3. Cambridge University Press, 2013.
- [9] T. Sondergaard and P. F. Lermusiaux, “Data assimilation with gaussian mixture models using the dynamically orthogonal field equations. part i: Theory and scheme,” *Monthly Weather Review*, vol. 141, no. 6, pp. 1737–1760, 2013.
- [10] T. Sondergaard and P. F. Lermusiaux, “Data assimilation with gaussian mixture models using the dynamically orthogonal field equations. part ii: Applications,” *Monthly Weather Review*, vol. 141, no. 6, pp. 1761–1785, 2013.
- [11] M. A. Iglesias, K. J. Law, and A. M. Stuart, “Ensemble kalman methods for inverse problems,” *Inverse Problems*, vol. 29, no. 4, p. 045001, 2013.
- [12] T. P. Sapsis and P. F. Lermusiaux, “Dynamically orthogonal field equations for continuous stochastic dynamical systems,” *Physica D: Nonlinear Phenomena*, vol. 238, no. 23-24, pp. 2347–2360, 2009.
- [13] M. Ueckermann, P. F. Lermusiaux, and T. P. Sapsis, “Numerical schemes for dynamically orthogonal equations of stochastic fluid and ocean flows,” *Journal of Computational Physics*, vol. 233, pp. 272–294, 2013.